Structures of plant viruses from vibrational circular dichroism

Ganesh Shanmugam,[1] Prasad L. Polavarapu,[1] Amy Kendall[2] and Gerald Stubbs[2]

Department of Chemistry[1] and Department of Biological Sciences[2], Vanderbilt University, Nashville, TN 37235, USA

Correspondence
Prasad L. Polavarapu
Prasad.L.Polavarapu@Vanderbilt.Edu

Received 22 March 2005
Accepted 10 May 2005

Vibrational circular dichroism (VCD) spectra in the amide I and II regions have been measured for viruses for the first time. VCD spectra were recorded for films prepared from aqueous buffer solutions and also for solutions using D_2O buffers at pH 8. Investigations of four filamentous plant viruses, *Tobacco mosaic virus* (TMV), *Papaya mosaic virus*, *Narcissus mosaic virus* (NMV) and *Potato virus X* (PVX), as well as a deletion mutant of PVX, are described in this paper. The film VCD spectra of the viruses clearly revealed helical structures in the virus coat proteins; the nucleic acid bases present in the single-stranded RNA could also be characterized. In contrast, the solution VCD spectra showed the characteristic VCD bands for α-helical structures in the coat proteins but not for RNA. Both sets of results clearly indicated that the coat protein conformations are dominated by helical structures, in agreement with earlier reports. VCD results also indicated that the coat protein structures in PVX and NMV are similar to each other and somewhat different from that of TMV. The present study demonstrates the feasibility of measuring VCD spectra for viruses and extracting structural information from these spectra.

INTRODUCTION

A variety of different spectroscopic and diffraction techniques have been used for structural analyses of viruses. These techniques include electronic circular dichroism (ECD) in the UV-visible region, vibrational Raman optical activity (ROA), crystallography for spherical viruses and fibre diffraction for filamentous viruses. While crystallography and fibre diffraction have the potential to provide complete descriptions of virus structures, they depend on the availability of virions at high purity and in relatively large quantities, and the formation of well-ordered crystals or fibres. They are therefore often not practical sources of structural information. The spectra structure correlation in ECD spectroscopy depends on observing characteristic ECD bands associated with a particular structure (Homer & Goodman, 1975; Erickson *et al.*, 1981). For proteins, such correlation can sometimes be misleading because of the overlap of ECD bands originating from the peptide backbone with those from aromatic groups. Specifically for viruses, differential light scattering, which is proportional to the fourth power of incident wavelength, can interfere with ECD bands. Furthermore, ECD spectroscopy is known to yield artefact signals when film samples are studied. ROA spectroscopy (Barron, 2004; Blanch *et al.*, 2002) is ideal for aqueous solution samples, but fluorescence interference and the requirement for higher concentrations pose limitations in some cases. Also it has not yet been possible to undertake ROA spectroscopy for film samples. The abovementioned limitations can be avoided with vibrational circular dichroism (VCD) spectroscopy.

VCD is a measure of the difference in absorption for left and right circularly polarized light in the infrared (IR) region (Keiderling, 1981; Nafie, 1984; Polavarapu, 1998; Barron, 2004). It is a useful method for studying the conformation of biomolecules in different environments and has therefore been used to investigate the structures of peptides, polypeptides and proteins in solution (Baumruk & Keiderling, 1993; Yoder *et al.*, 1995; Kocak *et al.*, 1998; Zhao & Polavarapu, 1999; Schweitzer-Stenner *et al.*, 2003; Shanmugam & Polavarapu, 2004a, b, c). The predominant secondary structure of a peptide or protein, such as α-helix, β-sheet or random coil, is reflected in the unique signs and/or patterns of the VCD bands that appear for the amide I (mainly due to peptide C=O stretching) and the amide II (mainly due to peptide N–H deformation) vibrations. The amide I vibrations appear in the 1750–1600 cm^{-1} region while amide II vibrations appear in the 1600–1500 cm^{-1} region. Several reports have discussed in detail the characteristic VCD features for these secondary structural components (Pancoska *et al.*, 1991; Shanmugam & Polavarapu, 2004a). Briefly, a right-handed α-helical structure exhibits a positive VCD couplet (a positive VCD band on the lower wave number side and a negative VCD band on the higher wave number side) in the amide I region and a

small negative VCD band in the amide II region. The random coil VCD spectrum has a negative VCD couplet in the amide I region, where a stronger negative band appears at a lower wave number and a positive band appears at a higher wave number (opposite to that seen in a right-handed α-helix). A β-sheet structure exhibits a small negative VCD band near 1620 cm^{-1} (amide I) and a negative VCD couplet in the amide II region. Characteristic VCD patterns in the amide I region for the 3_{10}-helix, β-turn and polyproline II structures have also been reported (Zhao *et al.*, 2000; Silva *et al.*, 2002).

Since water absorbs strongly in the infrared region, it is not a favourable solvent for IR absorption and VCD spectroscopy. One approach to overcoming this limitation is to use higher sample concentrations and minimize the interference from solvent absorption. An alternative is to use other solvents, such as D_2O or DMSO, although these solvents may not reflect physiological environments. Using one or both of these options, several VCD reports have been published for peptides, proteins, nucleic acids and carbohydrates in solution (Annamalai & Keiderling, 1987; Tummalapalli *et al.*, 1988; Bose & Polavarapu, 1999a, b; Zhao *et al.*, 2000; Shanmugam & Polavarapu, 2004b, c). The need for higher concentrations when aqueous solutions are used has been a limiting factor for applications of VCD to biological systems. Another limitation for measurements in D_2O solvent is that only the protons on exposed amide groups may exchange for deuterium, while the buried amide protons may not. A different approach to overcoming these limitations is to deposit aqueous solutions as films and undertake studies on films. As most of the solvent is dried out in preparing the films, solvent absorption interference is no longer a problem. In addition, dilute stock solutions can be used to prepare the films for investigation, so concentration limitations are not as troubling. The film VCD spectra generally have better signal-to-noise ratios than the corresponding spectra for solutions because of increased light transmission. VCD measurements performed on films of proteins (Shanmugam & Polavarapu, 2004a) and carbohydrates (Petrovic *et al.*, 2004) have been reported recently. Also, thermally induced structural changes in bovine serum albumin have been reported using the film method (Shanmugam & Polavarapu, 2004b). The ability to record VCD spectra for films opens up opportunities for applying this method to many biological systems, including viruses.

VCD spectral studies on viruses have not been reported before now. In this paper, we report the first measurement of VCD spectra in the amide I and II regions for viruses in the form of films derived from dilute aqueous buffer solutions. For comparative studies, we also measured VCD spectra of viruses in solution. Four filamentous plant viruses, *Tobacco mosaic virus* (TMV), *Papaya mosaic virus* (PMV), *Potato virus X* (PVX) and *Narcissus mosaic virus* (NMV), were investigated. In addition, we investigated a deletion mutant of PVX (PVX-Δ21). TMV belongs to the genus *Tobamovirus* comprising rigid, rod-shaped, helical plant viruses (Lewandowski & Dawson, 1999), approximately 3000 Å (300 nm) long and 180 Å (18 nm) in diameter. Tobamoviruses contain single-stranded positive-sense RNA. The detailed structure of TMV has been determined by X-ray fibre diffraction (Namba *et al.*, 1989). PVX, PMV and NMV are members of the genus *Potexvirus* (AbouHaidar & Gellatly, 1999), comprising flexuous filamentous viruses about 5000 Å (500 nm) long and 140 Å (14 nm) in diameter, also containing single-stranded positive-sense RNA. Previous studies using X-ray fibre diffraction, ROA and ECD have shown that the protein structures in these viruses are dominated by α-helices (Homer & Goodman, 1975; Erickson *et al.*, 1981; Namba *et al.*, 1989; Wilson *et al.*, 1991; Orlov *et al.*, 2001; Blanch *et al.*, 2002).

Our VCD results also suggested that the coat proteins of these viruses contain α-helices, both in film and in solution. The structures of PVX and NMV were found to be similar to each other, as expected, but different from TMV. Although the viral RNA could not be detected by VCD measurements in solution, the film VCD spectra showed characteristics of both nucleic acid and protein. Our results demonstrate the usefulness of VCD in the structural analysis of viruses and provide new structural information. The VCD spectra of PVX and NMV suggest that both the coat protein and RNA structures are extremely similar for these two viruses, based on the VCD band positions and sign patterns. Furthermore, the presence of small amounts of β-sheet conformation in PVX and NMV was clearly demonstrated; previous reports of β structure in these viruses have been ambiguous. The secondary structure of the coat protein was similar in solution and dried (film) states for the viruses studied here, except for the mutant virus PVX-Δ21.

METHODS

Viruses. TMV was purified (Boedtker & Simmons, 1958) from *Nicotiana tabacum*, var. Samsun. NMV was purified (Goodman, 1975) from *Chenopodium quinoa*. PMV was purified (Erickson & Bancroft, 1978) from *Carica papaya* var. Mexican. PVX was purified (Parker *et al.*, 2002) from *Nicotiana clevelandii*. The inoculum for PVX-Δ21 was a gift from Dr Simon Santa Cruz (Scottish Crop Research Institute, Dundee, Scotland, UK), made by deleting residues 2–22 from PVX (Chapman *et al.*, 1992). The mutant virus was purified (Parker *et al.*, 2002) from *N. clevelandii*. All of the potexvirus purifications included the addition of protease inhibitors (Parker *et al.*, 2002).

For solution VCD spectra, viruses were centrifuged and resuspended twice in D_2O buffers. The first centrifugation was for 1 h at 100 000 ***g***; the second for 1 h at 150 000 ***g***.

VCD study. All VCD spectra were recorded on a commercial Chiralir spectrometer (Bomem-Bio Tools) modified to minimize artefacts using the double polarization modulation method (Nafie, 2000). Details of the modification of the VCD instrument have been published previously (Shanmugam & Polavarapu, 2004a). Film and

Table 1. Concentrations and buffers used for experimental measurements

Viruses	Approximate concentration (mg ml^{-1})*		Buffer solutions
	Solution	Film	
TMV	5	8·5	25 mM Tris/HCl, pH 8
PMV	5	5	5 mM Tris/HCl, pH 8
PVX	7	7	10 mM Tris/HCl/5mM EDTA, pH 8
NMV	3·5	5	10 mM Tris/HCl/5mM EDTA, pH 8
PVX-Δ21	5	7·5, 5, 2·5	10 mM Tris/HCl/5mM EDTA, pH 8

*For films these concentrations refer to the stock solutions used to prepare films.

solution VCD spectra were collected for 1 and 3 h, respectively, at a resolution of 8 cm^{-1}. Virus concentrations and buffer solutions used for solution and film state measurements are given in Table 1.

For film measurements, approximately 100–150 μl of the stock solution was placed on a 2·5 cm diameter CaF_2 window that was placed in a fume hood to provide a constant air flow over the sample. Evaporation was continued (approx. 1–2 h) at room temperature until a dry thin film formed on the CaF_2 window. The homogeneity of the films was tested by a comparison of the VCD spectra obtained from the film rotated by 45° around the light beam axis. For all of the film VCD data reported here, the VCD band signs and positions were reproduced upon 45° rotation of the film. Baseline corrections were made by subtracting the VCD spectrum of a blank CaF_2 window obtained under the same conditions as the sample spectrum. For solution VCD spectra, the virus samples were prepared in D_2O buffers at pH 8. The virus stock solutions were placed between two CaF_2 windows separated by a 100 μm spacer (50 μm in the case of PVX-Δ21). For solution ECD spectra, a quartz cell with a 0·1 mm path length was used.

RESULTS AND DISCUSSION

VCD and vibrational absorption spectra of TMV, PMV, PVX and NMV virus films obtained from aqueous buffer solutions at pH 8 are presented in Fig. 1(a). In order to analyse the VCD data, we made use of the correlations established for the VCD spectral features of proteins and RNA in solution (Annamalai & Keiderling, 1987; Gupta & Keiderling, 1992; Baumruk & Keiderling, 1993; Shanmugam & Polavarapu, 2004a). VCD of TMV showed an intense negative band at 1660 cm^{-1} followed by a weak positive band at 1639 cm^{-1} and a negative band at 1517 cm^{-1}. The former two bands originated from protein amide I vibrations involving mainly C=O stretching, characteristic of α-helical proteins. The latter originated from the amide II vibrations involving protein backbone N–H deformations. Both features are characteristic of α-helical proteins (Shanmugam & Polavarapu, 2004a). The virus structure includes a single strand of RNA surrounded by a helical array of coat protein subunits. The VCD bands from the RNA were expected to be much weaker than from the proteins owing to the low RNA content (~6%). Nevertheless, the weak negative VCD band seen at 1685 cm^{-1} for TMV may have arisen from the RNA bases, since nucleic acids often show VCD in these regions. More specifically, these bands may have originated from guanine, since bands at similar wave numbers assigned to this base are seen in the VCD spectrum of polyguanine (Annamalai & Keiderling, 1987). It has been shown that all polynucleotides give a positive VCD couplet (bisignate pattern with a negative band on the higher and a positive band on the lower energy side) centred at their corresponding IR absorption maxima

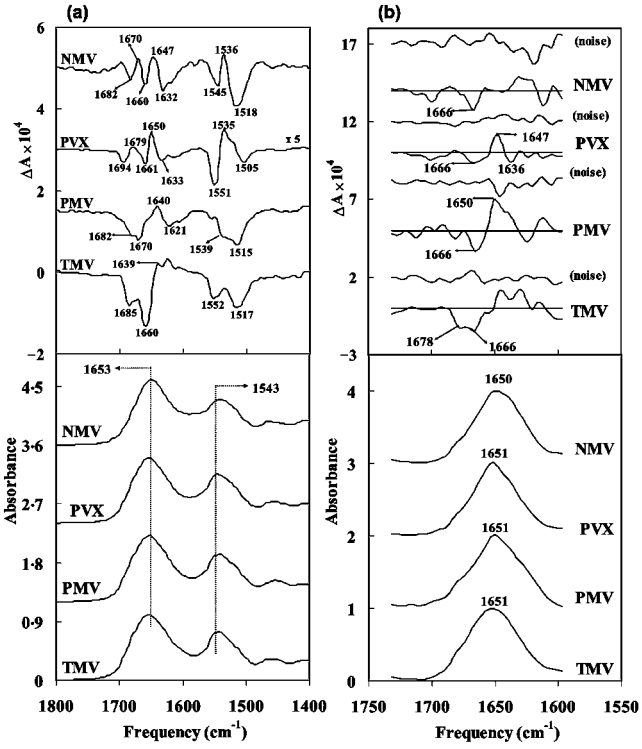

Fig. 1. VCD (top) and vibrational absorption (bottom) spectra of TMV, PMV, PVX and NMV. Films obtained from aqueous buffers (a) and in D_2O buffer (pH 8) (b) at concentrations of 5–10 mg ml^{-1} (see Table 1 for details). The corresponding noise spectra obtained for solution VCD are shown above each spectrum. Data collection times were 1 and 3 h for film and solution measurements, respectively, at a resolution of 8 cm^{-1}. Path length was 100 μm for solution measurements. The film spectrum of PVX was scaled by 0·2 to keep it on the scale.

(Annamalai & Keiderling, 1987) between 1720 and 1600 cm^{-1}. In the present case, the positive VCD band in the positive couplet of guanine could not be observed because a negative VCD band from a strong α-helical protein component occurred at the same position. The corresponding IR absorption spectrum of TMV showed single, broad, intense amide I and II bands at 1653 and 1543 cm^{-1}, confirming the presence of an α-helical structure (Shanmugam & Polavarapu, 2004a).

In the case of PMV, a positive VCD couplet (negative component at 1670 cm^{-1} and positive component at 1640 cm^{-1}) in the amide I region and a negative band in the amide II region at 1515 cm^{-1} appeared (Fig. 1a). The presence of these bands suggested an α-helical structure for PMV. A weak negative band at a lower frequency (1621 cm^{-1}) was also seen for PMV, suggesting some β structure (Baumruk & Keiderling, 1993). The presence of a weak band at 1682 cm^{-1} may have originated from RNA bases, as observed in the case of TMV (Fig. 1a). Thus, the VCD spectra of TMV and PMV were seen to be dominated by protein bands. The corresponding IR absorption spectra of PMV and all other viruses from the genus *Potexvirus* (see below) examined here showed single, broad, intense amide I and II bands at 1653 and 1543 cm^{-1}, confirming the presence of α-helical structures (Shanmugam & Polavarapu, 2004a).

Our VCD data are consistent with previous results from proteins containing α-helical structures. The coat protein subunits were seen to have a large proportion of α-helical structure; in the case of TMV, this structure is known to be in the form of a four-helix bundle containing both water-exposed residues and residues at hydrophilic and hydrophobic helix–helix interfaces (Namba *et al.*, 1989). Furthermore, far-UV CD and ROA results predicted a high proportion of helical structure in aqueous solution (Orlov *et al.*, 2001; Blanch *et al.*, 2002).

The VCD and vibrational absorption spectra of PVX and NMV films are shown in Fig. 1(a, top two spectra). The overall appearances of the VCD spectra of PVX and NMV were very similar, particularly between 1700 and 1600 cm^{-1}, indicating that the structures of these two viruses are similar. The VCD spectrum of PVX showed a positive couplet (a negative band at 1661 cm^{-1} followed by a positive band at 1650 cm^{-1}) characteristic of an α-helical structure. This interpretation was confirmed by the negative amide II band at 1505 cm^{-1}, also characteristic of a helical structure. The presence of an additional negative band at 1633 cm^{-1} indicated that β-sheet structure was also present in the film state. The presence of another positive couplet on the higher energy side (a negative band at 1694 cm^{-1} and a positive band at 1679 cm^{-1}) is characteristic of nucleic acid bases, particularly guanine. The VCD spectrum of NMV showed a positive VCD couplet (negative at 1660 cm^{-1} and positive at 1647 cm^{-1}) and a weak negative band at 1632 cm^{-1}, all similar to those of PVX, except for small shifts in band positions. The VCD spectra also showed a 'W' pattern between 1600 and 1500 cm^{-1} (a negative band at 1505–1518 cm^{-1} and a positive band at 1536 cm^{-1} followed by a negative band at 1545–1551 cm^{-1}), which was similar for both PVX and NMV, except for changes in the relative intensities of the individual components. The VCD bands due to nucleic acid bases were also seen for NMV at 1670 (positive) and 1682 (negative) cm^{-1}, similar to those for PVX. Thus, unlike TMV and PMV, the spectra of PVX and NMV in the film state clearly showed bands that were characteristic of both coat protein and nucleic acid bases. It is premature to suggest structures for the nucleic acid from the limited number of VCD observations reported here, but with more VCD investigations on viruses in the future it might be possible to infer the structures of nucleic acids in viruses.

ROA data indicate that PVX and NMV in aqueous solution contain α-helical and hydrated β structures (Blanch *et al.*, 2002). However, UV CD data predict large amounts of α-helix but little β-sheet structure (Homer & Goodman, 1975; Wilson *et al.*, 1991). Our results indicated the presence of β structures in PVX and NMV. For the PVX coat protein, Baratova *et al.* (1992) predicted from the amino acid sequence a coat protein structure that included a well-defined β structure at both the N- and C-terminal ends of the protein. Sawyer *et al.* (1987) suggested that the N-terminal 50 residues of PVX have zero probability of having an α-helical structure. Our VCD results confirm the presence of both α-helical and β-sheet structures in the PVX and NMV coat proteins.

There is no similarity in the amino acid sequences of TMV and the potexvirus coat proteins. Our results clearly suggest that there is some difference between the structures of TMV and the potexviruses. VCD has provided evidence for helical structures in all of the viruses and some β-sheet structures in PVX, NMV and PMV, but not in TMV. It has been suggested (Sawyer *et al.*, 1987; Shukla *et al.*, 1988; Blanch *et al.*, 2002) that the coat protein folds of PVX and NMV may be similar to that of TMV, being based on the helix bundle, but with differences in detail resulting from differences in the appended loops and turns and from the extra sequences present in the potexviruses. These differences may be responsible for the observed VCD differences.

For comparative studies, we also measured the VCD and vibrational absorption spectra of TMV, PMV, PVX and NMV in D_2O buffer solution at pH 8. It should be noted that, unlike the situation in film measurements, the absorption background from D_2O precludes observations in the amide II region. Furthermore, the signal-to-noise ratio is lower in solution than in film, owing to the lower amount of light transmitted through D_2O solutions. The solution spectra are shown in Fig. 1(b). Both TMV and PMV in Tris buffer at pH 8 (Table 1) showed a positive VCD couplet (a negative band at 1666 cm^{-1} and a positive band at 1650 cm^{-1}) characteristic of a helical structure. The negative band in this couplet was slightly shifted relative to the corresponding couplet in the film VCD. A weak negative

VCD band at 1624 cm^{-1} for PMV was associated with a β-sheet structure, as in the film VCD. This β-sheet VCD band was not seen for TMV. These data suggest that the virus coat protein structures did not change significantly between the solution and film states for PMV and TMV. The vibrational absorption spectra in Fig. 1(b) also showed the characteristic helical amide I band at 1651 cm^{-1} for TMV and PMV.

The VCD spectrum of PVX in Tris/EDTA buffer at pH 8 (Fig. 1b) showed diagnostic bands for an α-helical structure (a positive couplet between 1640 and 1670 cm^{-1}). Furthermore, the spectrum had a weak negative VCD band in the β-sheet region (1636 cm^{-1}), as observed for PVX film (Fig. 1a). A weak positive couplet in the higher frequency region (not marked in the spectrum) could be due to nucleic acid bases. For NMV, the low concentration of the virus sample resulted in a lower signal quality. Nevertheless, the solution VCD spectrum of NMV (Fig. 1b) revealed features similar to those of PVX. The positive VCD band at $\sim$1640 cm^{-1} was quite weak and was not seen clearly above the noise. The vibrational absorption spectra of PVX and NMV clearly showed the characteristic helical band centred at $\sim$1651 cm^{-1} (Fig. 1b, bottom). These results suggested that there is no significant change in the protein structure of PVX and NMV between aqueous buffer solution and films derived from the same buffer solution, although the quality of the VCD spectra was better in film than in solution.

The VCD spectra of the viruses in solution were dominated by protein bands, unlike the film VCD spectra in which bands due to RNA were also observed. The VCD bands from the RNA were expected to be much weaker than those from the protein because of the low RNA content ($\sim$6%). Even though the concentrations of virus samples used for film and solution studies were approximately the same, VCD clearly showed characteristic nucleic acid bands in the film state but not in solution. This result indirectly confirmed our conclusion that the positive couplet observed for different viruses between 1670 and 1635 cm^{-1} in the film VCD spectra was from the peptide backbone carbonyl stretching and not from the nucleic acid bases.

We also measured the VCD spectra of a deletion mutant of PVX (PVX-Δ21), from which residues 2–22 of the wild-type coat protein had been removed. Spectra were measured both in solution and in the film state to investigate the conformational differences (if any) between PVX-Δ21 and PVX. The film VCD spectrum of PVX-Δ21 was significantly different from that of PVX (Fig. 2a). The VCD spectrum of PVX-Δ21 film showed a single negative band centred at 1651 cm^{-1} in the amide I region, indicative of an α-helical structure. However, for an α-helical structure there should also be a positive VCD band on the lower frequency side of the 1651 cm^{-1} negative VCD. This positive band did not appear in the film VCD spectrum. The presence of a negative VCD band at 1521 cm^{-1} (amide II) in the film VCD of PVX-Δ21 also suggested a helical structure. The film VCD spectrum of PVX-Δ21 did not show any characteristic

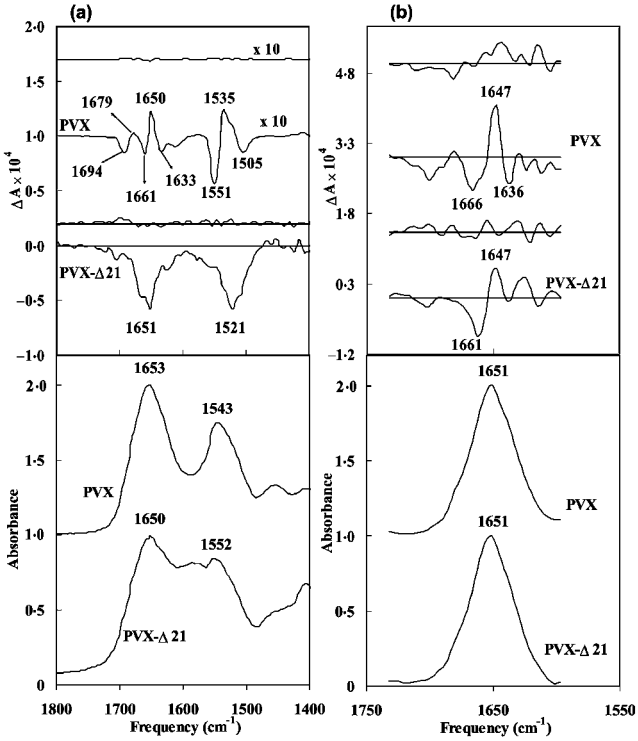

Fig. 2. VCD (top) and vibrational absorption (bottom) spectra of PVX-Δ21 and PVX in 10 mM Tris/HCl, 5 mM EDTA (pH 8) for film (a) and in solution (b). For details of concentrations used, see Table 1 (the film spectrum shown for PVX-Δ21 was obtained for the film prepared from a stock solution of $\sim$2·5 mg ml^{-1}). The data collection time was 3 h and resolution was 8 cm^{-1}. A path length of 50 μm was used for solution VCD. The VCD spectra of PVX for film and in solution are reproduced here for comparison, from Fig. 1. The noise associated with each spectrum is presented above the corresponding VCD spectrum. The film spectrum of PVX and the associated noise were scaled by 0·1.

band for the nucleic acid bases, unlike the film VCD of PVX. In order to eliminate the possibility of artefacts in the film VCD of mutant PVX, we repeated the VCD measurements with films prepared from stock solutions of three different concentrations (see Table 1); in all cases the same VCD features were obtained. In addition, the film VCD was found to be independent of film orientation when the film was rotated around the light beam axis. These tests led us to believe that the film VCD spectra for mutant PVX did not contain artefacts. Fig. 2(b) compares the VCD (top) and vibrational absorption (bottom) spectra of PVX-Δ21 and PVX in D_2O buffer, pH 8. For comparison, the corresponding noise spectrum is presented above the VCD spectrum. Only those VCD bands that had magnitudes $>0{\cdot}5\times10^{-5}$ are discussed here, since the noise level in the VCD spectra was $\sim0{\cdot}5\times10^{-5}$. The observed VCD spectrum of PVX-Δ21 clearly showed the positive couplet (negative band at 1661 cm^{-1} and positive band at 1647 cm^{-1}) and the absorption spectrum showed an absorption maximum at

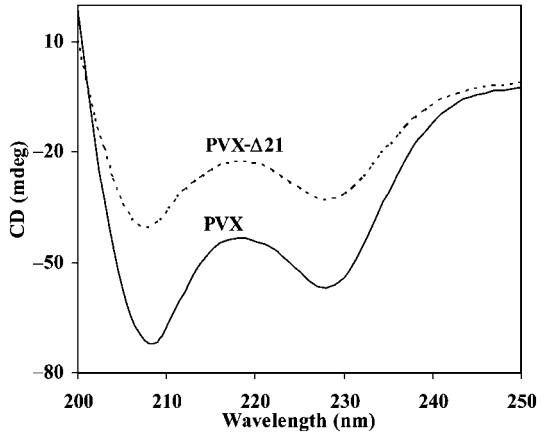

Fig. 3. ECD spectra of PVX and PVX-Δ21 in 10 mM Tris/HCl, 5 mM EDTA (pH 8). Concentrations of PVX and PVX-Δ21 were ~7 and ~2·5 mg ml^{-1}. The path length of the quartz cell was 0·1 mm.

1651 cm^{-1}, indicating an α-helical structure similar to that of PVX. This result suggested that in solution the coat protein structure of PVX-Δ21 is not significantly different from that of wild-type PVX.

The difference between the film and solution VCD spectra for PVX-Δ21 suggested a conformational change during film formation and/or that the nature of the film formed by PVX-Δ21 was significantly different from that of PVX. The absorption spectra obtained for PVX-Δ21 in solution and as film were also significantly different, unlike that for PVX (Fig. 2). In order to examine further the conformation of PVX-Δ21, we measured ECD spectra for PVX-Δ21 and PVX under similar conditions. The ECD spectra of PVX and PVX-Δ21 in 10 mM Tris/HCl, 5 mM EDTA buffer (pH 8) are shown in Figure 3. From this figure, it is clear that the viruses have similar ECD spectra, with negative double minima at 208 and 228 nm due to $\pi \rightarrow \pi^*$ and $n \rightarrow \pi^*$ transitions, respectively, which are characteristic of proteins adopting α-helical structures in solution. The observed $n \rightarrow \pi^*$ transition band was slightly red-shifted from the normal helix CD band (222 nm), because of the presence of aromatic amino acid residues in the proteins. The ECD results, like the VCD results in solution, demonstrated that the structure of PVX in solution did not change after the removal of ~20 aa from the N-terminal end of the coat protein. However, the differences in the VCD spectra of films of the wild-type and the mutant virus indicated that there were structural differences under these conditions, presumably because the mutant structure is less robust and is affected by drying.

Conclusion

We used VCD, a relatively new spectroscopic technique, to probe the structures of viruses under two different conditions. We have presented the VCD spectra of several viruses in both film and solution states for the first time. This work demonstrated the measurability of the amide I and II VCD bands for films and amide I VCD bands in D_2O buffer solutions for viruses. Furthermore, qualitative correlation with the secondary structural characteristics, as previously reported in solution using ROA, UV CD and X-ray fibre diffraction methods, has been demonstrated. The VCD spectra in solution and in film suggest a predominantly α-helical structure for the coat proteins of these viruses. The results also suggest that the coat protein folds of PVX and NMV are similar to each other and are somewhat different from that of TMV in film state. This result clarifies some previous ambiguities in structure comparisons of PVX, NMV and TMV. Film VCD spectra provide information about the nucleic acid structure in the viruses, even though this information is not available from VCD in solution.

ACKNOWLEDGEMENTS

This material is based upon work supported by the National Science Foundation (#0092922 to P. L. P. and #0235653 to G. Stubbs.). We thank Ian McCullough for assistance with virus purification and Dr Simon Santa Cruz for the PVX mutant virus inoculum.

REFERENCES

AbouHaidar, M. G. & Gellatly, D. (1999). Potexviruses. In *Encyclopedia of Virology*, 2nd edn, pp. 1364–1368. Edited by A. Granoff & R. G. Webster. London: Academic Press.

Annamalai, A. & Keiderling, T. A. (1987). Vibrational circular dichroism of polyribonucleic acids. A comparative study in aqueous solution. *J Am Chem Soc* **109**, 3125–3132.

Baratova, L. A., Grebenshchikov, N. I., Dobrov, E. N. & 7 other authors (1992). The organization of potato virus X coat proteins in virus particles studied by tritium planigraphy and model building. *Virology* **188**, 175–180.

Barron, L. D. (2004). *Molecular Light Scattering and Optical Activity*, 2nd edn. London: Cambridge University Press.

Baumruk, V. & Keiderling, T. A. (1993). Vibrational circular dichroism of proteins in H_2O solution. *J Am Chem Soc* **115**, 6939–6942.

Blanch, E. W., Robinson, D. J., Hecht, L., Syme, C. D., Nielsen, K. & Barron, L. D. (2002). Solution structures of potato virus X and narcissus mosaic virus from Raman optical activity. *J Gen Virol* **83**, 241–246.

Boedtker, H. & Simmons, N. S. (1958). The preparation and characterization of essentially uniform tobacco mosaic virus particles. *J Am Chem Soc* **80**, 2550–2556.

Bose, P. K. & Polavarapu, P. L. (1999a). Vibrational circular dichroism of monosaccharides. *Carbohyd Res* **319**, 172–183.

Bose, P. K. & Polavarapu, P. L. (1999b). Acetate groups as probes of the stereochemistry of carbohydrates: a vibrational circular dichroism study. *Carbohyd Res* **322**, 135–141.

Chapman, S., Hills, G., Watts, J. & Baulcombe, D. (1992). Mutational analysis of the coat protein gene of potato virus X: effects on virion morphology and viral pathogenicity. *Virology* **191**, 223–230.

Erickson, J. W. & Bancroft, J. B. (1978). The self-assembly of papaya mosaic virus. *Virology* **90**, 36–46.

Erickson, J. W., Bancroft, J. B. & Stillman, M. J. (1981). Circular dichroism studies of papaya mosaic virus coat protein and its polymers. *J Mol Biol* **147**, 337–349.

Goodman, R. M. (1975). Reconstitution of potato virus X *in vitro*. I. Properties of the dissociated protein structural subunits. *Virology* **68**, 287–298.

Gupta, V. P. & Keiderling, T. A. (1992). Vibrational CD of the amide II band in some model polypeptides and proteins. *Biopolymers* **32**, 239–248.

Homer, R. B. & Goodman, R. M. (1975). Circular dichroism and fluorescence studies on potato virus X and its structural components. *Biochim Biophys Acta* **378**, 296–304.

Keiderling, T. A. (1981). Vibrational circular dichroism. *Appl Spectrosc Rev* **17**, 189–225.

Kocak, A., Luque, R. & Diem, M. (1998). The solution structure of small peptides: an infrared CD study of aqueous solutions of (L-Ala)$_n$ [n=3, 4, 5, 6] at different temperatures and ionic strengths. *Biopolymers* **46**, 455–463.

Lewandowski, D. J. & Dawson, W. O. (1999). Tobamoviruses. In *Encyclopedia of Virology*, 2nd edn, pp. 1780–1783. Edited by A. Granoff & R. G. Webster. London: Academic Press.

Nafie, L. A. (1984). Experimental and theoretical advances in vibrational optical activity. In *Advances in Infrared and Raman Spectroscopy*, vol. 11, pp. 49–93. Edited by R. J. H. Clark & R. E. Hester. London: Heyden & Sons.

Nafie, L. A. (2000). Dual polarization modulation: a real-time, spectral-multiplex separation of circular dichroism from linear birefringence spectral intensities. *Appl Spectrosc* **54**, 1634–1645.

Namba, K., Pattanayek, R. & Stubbs, G. (1989). Visualization of protein–nucleic acid interactions in a virus; refinement of intact tobacco mosaic virus structure at 2·9Å resolution by fiber diffraction. *J Mol Biol* **208**, 307–325.

Orlov, V. N., Arutyunyan, A. M., Kust, S. V., Litmanovich, E. A., Drachev, V. A. & Dobrov, E. N. (2001). Macroscopic aggregation of tobacco mosaic virus coat protein. *Biochemistry* **66**, 154–162.

Pancoska, P., Yasui, S. C. & Keiderling, T. A. (1991). Statistical analyses of the vibrational circular dichroism of selected proteins and relationship to secondary structures. *Biochemistry* **30**, 5089–5103.

Parker, L., Kendall, A. & Stubbs, G. (2002). Surface features of potato virus X from fiber diffraction. *Virology* **300**, 291–295.

Petrovic, A. G., Bose, P. K. & Polavarapu, P. L. (2004). Vibrational circular dichroism of carbohydrate films formed from aqueous solutions. *Carbohydr Res* **339**, 2713–2720.

Polavarapu, P. L. (1998). *Vibrational Spectra: Principles and Applications with Emphasis on Optical Activity*. New York: Elsevier Publications.

Sawyer, L., Tollin, P. & Wilson, H. R. (1987). A comparison between the predicted secondary structures of potato virus X and papaya mosaic virus coat proteins. *J Gen Virol* **68**, 1229–1232.

Schweitzer-Stenner, R., Eker, F., Perez, A., Griebenow, K., Cao, X. & Nafie, L. A. (2003). The structure of tri-proline in water probed by polarized Raman, Fourier transform infrared, vibrational circular dichroism, and electric ultraviolet circular dichroism spectroscopy. *Biopolymers* **71**, 558–568.

Shanmugam, G. & Polavarapu, P. L. (2004a). Vibrational circular dichroism of protein films. *J Am Chem Soc* **126**, 10292–10295.

Shanmugam, G. & Polavarapu, P. L. (2004b). Structure of Aβ(25-35) peptide in different environments. *Biophys J* **87**, 622–630.

Shanmugam, G. & Polavarapu, P. L. (2004c). Vibrational circular dichroism spectra of protein films: thermal denaturation of bovine serum albumin. *Biophys Chem* **111**, 73–77.

Shukla, D. D., Strike, P. M., Tracy, S. L., Gough, K. H. & Ward, C. W. (1988). The N and C termini of the coat proteins of potyviruses are surface-located and the N terminus contains the major virus specific epitopes. *J Gen Virol* **69**, 1497–1508.

Silva, R. A., Yasui, S. C., Kubelka, J., Formaggio, F., Crisma, M., Toniolo, C. & Keiderling, T. A. (2002). Discriminating 3_{10}-from α-helices: vibrational and electronic CD and IR absorption study of related Aib-containing oligopeptides. *Biopolymers* **65**, 229–243.

Tummalapalli, C. M., Back, D. M. & Polavarapu, P. L. (1988). Fourier-transform infrared vibrational circular dichroism of simple carbohydrates. *J Chem Soc Faraday Trans 1* **84**, 2585–2594.

Wilson, H. R., Tollin, P., Sawyer, L., Robinson, D. J., Price, N. C. & Kelly, S. M. (1991). Secondary structures of narcissus mosaic virus coat protein. *J Gen Virol* **72**, 1479–1480.

Yoder, G., Keiderling, T. A., Formaggio, F., Crisma, M. & Toniolo, C. (1995). Characterization of β-bend ribbon spiral forming peptides using electronic and vibrational CD. *Biopolymers* **35**, 103–111.

Zhao, C. & Polavarapu, P. L. (1999). Vibrational circular dichroism is an incisive structural probe: ion-induced structural changes in gramicidin D. *J Am Chem Soc* **121**, 11259–11260.

Zhao, C., Polavarapu, P. L., Das, C. & Balaram, P. (2000). Vibrational circular dichroism of β-hairpin peptides. *J Am Chem Soc* **122**, 8228–8231.